

# INDOOR POSITIONING METHOD BASED ON SINGLE BASE STATION AUDIO SIGNAL

JingSong Liang<sup>1,2</sup>, Liang Chen<sup>1,2\*</sup>

<sup>1</sup> State Key Laboratory of Information Engineering in Surveying, Mapping and Remote Sensing, Wuhan University, Wuhan 430079, China

<sup>2</sup> HuBei Luojia Laboratory, Wuhan 430079, China

Commission III, WG III/1

**KEY WORDS:** internet of things technology(IoT), indoor positioning, audio signal, smartphones, signal strength.

## ABSTRACT:

The growth of the Internet of Things has increased demand for location information services, but existing indoor positioning technology has limitations. The purpose of this paper is to discuss indoor positioning with a single audio base station and to propose an indoor positioning method based on signal strength. The proposed method is simple to use on smart phones, and the base station is straightforward to deploy. The base station transmits digital amplitude modulated signals in multiple directions using this method. Prior to the test, a database is created with the signal strengths measured at multiple points throughout the area to be evaluated. During the test, the terminal measures the signal strength and compares it to the database to determine the spatial position. Indoor dynamic and static tests are conducted to evaluate the method's performance. The test results demonstrate that the positioning method is highly accurate and will meet the requirements for indoor location-based services.

## 1. INTRODUCTION

With the development of Internet of Things (IoT) technology, there is a huge demand for positioning services of indoor and outdoor (Chen et al., 2017). At present, outdoor positioning technology including Global Navigation Satellite System (GNSS) (Shen et al., 2022) (Shen et al., 2021), low earth orbit navigation augmentation (Chen et al., 2021a) and wireless positioning based on DVB-T (Liang et al., 2017) has been gradually improved. However, the development of indoor positioning technology is slow relatively (Chen and Chen, 2021). The current popular indoor positioning technologies include positioning technologies based on inertial measurement unit (IMU), geomagnetism (Al-homayani and Mahoor, 2018), electromagnetic waves and acoustic waves (Song et al., 2020). The IMU positioning technology has a drift problem. Without the assistance of other positioning technologies, the IMU cannot independently locate for a long time (Li et al., 2019). Geomagnetic positioning is easily disturbed by metal objects, so it is more difficult to use in practice. Electromagnetic field positioning technology includes ultra-wideband (UWB) positioning technology (Yao et al., 2017), wireless fidelity (WIFI) (Shilo et al., 2020) (Yu et al., 2022), 5th Generation Mobile Communication Technology (5G) (Chen et al., 2021b) and Bluetooth low energy (BLE) positioning technology (Pakanon et al., 2020) (Ji et al., 2022). These electromagnetic wave-based positioning technologies require special RF baseband chips for signal processing (Farahsari et al., 2022), so these positioning methods is limited to specific user terminals. The positioning technology based on audio waves has a wide range of applicability. Various IoT devices including smartphones that can receive audio signals directly. There are two main audio wave localization technologies, one is based on the microphone array audio source (Soda et al., 2011), and the other is based on the multi-audio source anchor point (Wang et al., 2015). In microphone array audio source localization technology system, The user terminal under test continuously sends audio signals, the microphone array receives the audio signals, and analyze and

calculate the terminal position and other information. Such positioning systems are very susceptible to interference from complex indoor environments. The multi-acoustic anchor positioning technology needs multiple base stations to transmit acoustic anchors at different positions in the area to be measured, which brings difficulties to the promotion of this technology.

In this paper, an indoor positioning method based on the signal strength of a single audio signal base station is proposed. In Figure 1, a signal transmitting base station that can transmit audio signals in different directions needs to be arranged in the middle of the test area. The user terminal under test receives audio signals in different directions sent by the base station. When the direction in which the base station transmits the audio signal is directly toward the terminal, the received audio signal has a higher strength, and vice versa. Based on this principle, the terminal processes the received signal from the base station to transmit in different directions to obtain the signal strength. Finally, the calculated signal strength is mapped to the spatial location information of the terminal. We will describe the proposed positioning method in terms of transmitter hardware, signal format, receiver signal processing flow, and indoor test results.

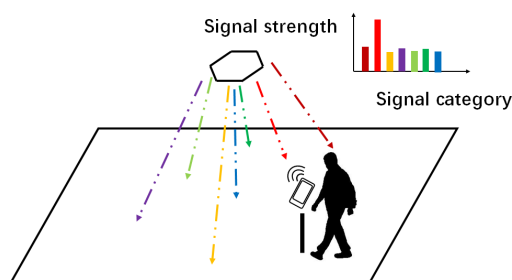


Figure 1. Indoor positioning method based on single base station audio signal

\* Corresponding author

## 2. THE AUDIO SIGNAL TRANSMITTING BASE STATION AND SIGNAL STRUCTURE

### 2.1 The Audio Signal Transmitting Base Station

Two pieces of hardware are required for the positioning system proposed in this paper. The base station transmits the audio signal, while the user terminal receives it. In this article, the receiving terminal is a common smartphone (MI10). The base station described in this paper has a total of seven audio directions, including one vertical and six oblique downward.

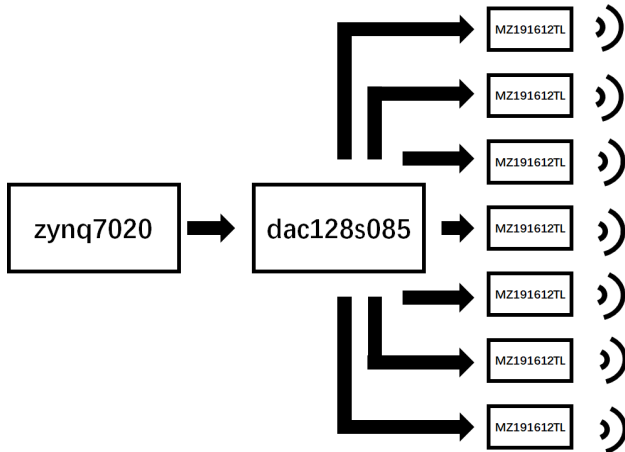


Figure 2. The topology of the hardware of the base station.

As depicted in Figure 2, the audio signal transmitting base station adopts the zynq7020 chip as the main control chip, the dac128s085 chip as the multi-channel signal output chip, and the audio signal transmitting probe MZ191612TL as the voltage audio converter. The zynq7020 is XILINX's soc type fpga, which has a dual-core ARM processor. The dac128s085 is a multi-channel dac from TI, and the sampling frequency of base station is 60Khz. MZ191612TL is a 19Khz acoustic piezoelectric signal transmitting probe from Manzekegi Company. The actual base station is presented in Figure 3.



Figure 3. (a)Internal circuit of the base station. (b) Outside of the base station.

### 2.2 Transmitting Signal Structure

When the user terminal is in the direct path of the signal, the signal strength will be greater, and vice versa. The user terminal receives and demodulates the audio signal transmitted by the base station, determines the strength of the audio signals, and finally determines the location of the user terminal.

To avoid interfering with audio signals transmitted in different directions, the base station's audio signals are specially designed.

In terms of baseband signals, the base station is equipped with a total of seven audio transmitters that transmit seven distinct 8-bit frames continuously. Each frame contains seven data bits and one stop bit. The frames are expressed as follows:

$$D_n = \begin{cases} [1, 0, 0, 0, 0, 0, 0, 0]^T, & n = 1; \\ [0, 1, 0, 0, 0, 0, 0, 0]^T, & n = 2; \\ [0, 0, 1, 0, 0, 0, 0, 0]^T, & n = 3; \\ [0, 0, 0, 1, 0, 0, 0, 0]^T, & n = 4; \\ [0, 0, 0, 0, 1, 0, 0, 0]^T, & n = 5; \\ [0, 0, 0, 0, 0, 1, 0, 0]^T, & n = 6; \\ [0, 0, 0, 0, 0, 0, 1, 0]^T, & n = 7. \end{cases} \quad (1)$$

where  $n$  = the number of the audio transmitter  
 $D_n$  = signal frame emitted by the nth audio transmitter.

Regarding signal modulation, the audio signal transmitted by the base station is binary amplitude keying (2ASK). Its center frequency is 19khz, and the baud rate is 4bit/s.

In time domain, the time length of each frame is 2 s, while the length of each bit is 0.25 s. According to Equation 1, the time domain representation of the frame is as follows:

$$X_n(t) = \begin{cases} \sin(2 \cdot \pi \cdot f_o \cdot t), & t \in (t_{bit} \cdot n, t_{bit} \cdot n + t_{bit}); \\ 0, & t \in [0, t_{bit} \cdot n] \cup [t_{bit} \cdot n + t_{bit}, t_{frame}]. \end{cases} \quad (2)$$

where  $t$  is time in seconds;  
 $X_n(t)$  = A frame waveform from transmitter n;  
 $t_{bit} = 0.25$ ;  
 $t_{frame} = 2.0$ ;  
 $f_o = 19e3$ .

According to Equations 1 and 2, as presented in Figure 4, when the bit sent by a transmitter in the data bit is 1 (that is, an audio signal is transmitted), the bits transmitted by the other transmitters are 0 (that is, no audio signal is transmitted). Such a signal structure ensures that the signals transmitted between the audio transmitters do not interfere with each other. The signals obtained by the receiver can be regarded as an amplitude-modulated (AM) waveform.

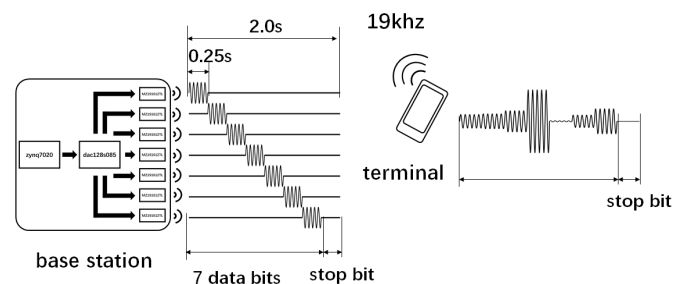


Figure 4. Audio signal transmission and reception.

## 3. THE SIGNAL PROCESSING FLOW OF THE USER TERMINAL FOR RECEIVING THE AUDIO SIGNAL

This section introduces the signal processing flow of the signal receiving user terminal, as illustrated in Figure 5. The process

includes calculating the spectrogram, framing, obtaining the signal strength, calculating the vector difference, and mapping.

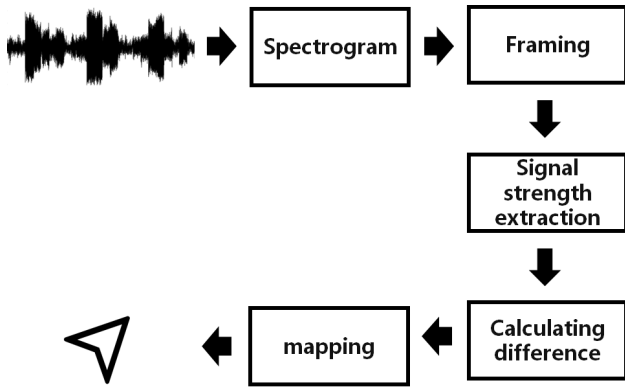


Figure 5. The signal processing flow of the user terminal.

### 3.1 Calculate the Audio Signal Spectrum

Spectrograms were generated from a short-time Fourier transform (STFT) using a 48Khz sampling rate, a window length of 2,048 samples, and an overlap of 1,748 sample points. The magnitude of the STFT produces a linear frequency  $S(m, t)$ , where  $k$  is the frequency interval between 1 and 1,025. In this work, frequency from  $k_{min} = 807$  to  $k_{max} = 819$  covering 19Khz were used for signal processing. Figure 6 shows the time-domain waveform and corresponding spectrogram of a signal that includes a complete frame and background noise.

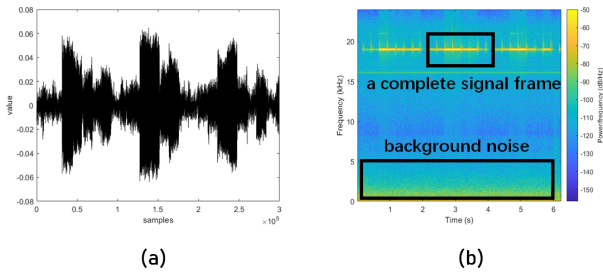


Figure 6. A segment of time-domain waveform and spectrum containing a complete frame of signal.

### 3.2 Audio Signal Framing

The framing step depends on the stop bit of each frame. The spectrum is processed by a sliding average window. When the result of the sliding average is less than the threshold  $th_{s_s}$ , the stop bit starts. According to Sections 2.2 and 3.1 of this paper, the formula for finding when the stop bit starts is as follows:

$$R(t) = \frac{1}{(k_{max} - k_{min}) \cdot t_{bit}} \cdot \sum_{t_0=t}^{t+t_{bit}} \sum_{k_0=k_{min}}^{k_{max}} S(k_0, t_0); R(t_s) < th_{s_s}. \quad (3)$$

where  $t$  = time in seconds  
 $R(t)$  = the moving average result  
 $S$  = Spectrograms  
 $t_s$  = time coordinate of the stop bit  
 $th_{s_s}$  = stop bit threshold.

According to Section 2.2 of this paper, the stop bit occupies the last 0.25 s of the 2 s of a complete frame. It means that the start time of a complete frame is  $t_{fs} = t_s - 1.75$ , while the end is  $t_{fe} = t_s + 0.25$

### 3.3 Obtaining the Strength of the Signal from Different Emission Angles

The 7-bit data bits of the signal at the receiver were provided by seven audio transmitters, respectively. According to Sections 3.1 and 3.2, the logarithmic expression of the signal strength of the audio from the seven transmitters can be obtained as follows:

$$P_n = \lg \left[ \frac{1}{(k_{max} - k_{min}) \cdot t_{bit}} \cdot \sum_{t=t_{fs}+0.25 \cdot (n-1)}^{t_{fs}+t_{bit} \cdot n} \sum_{k_0=k_{min}}^{k_{max}} S(k, t) \right] \quad (4)$$

where  $t$  = time in seconds  
 $P(n)$  = strength of the signal from transmitter  $n, n = 1, 2, \dots, 7$   
 $S$  = spectrograms  
 $t_{fs}$  = start of a full frame.

The signal strength vector of user terminal  $V_u$  can be obtained

$$V_u = [P_1, P_2, P_3, \dots, P_7]^T \quad (5)$$

### 3.4 Calculating the Vector Difference with the Database

The signal strength vector  $V_u$  can be calculated according to Section 3.3. In order to identify the signal characteristics of different regions. Database is collected and obtained from multiple locations within the test area.

$$D = \{V'_{d,f} | d = 1, 2, \dots, d_{max}; f = 1, 2, \dots, f_{max}\} \quad (6)$$

where  $V'_{d,f}$  = the  $f$ -th data at the  $d$ -th position;  
 $d_{max}$  = the number of measurement positions;  
in this paper, this value is equal to 35;  
 $f_{max}$  = the amount of data at the same location;  
in this paper, this value is equal to 7.

The difference between the signal strength vector and the database is measured as follows:

$$M_d = \frac{1}{f_{max}} \cdot \sum_{i=1}^{f_{max}} |V_u - V'_{d,i}|^2 \quad (7)$$

where  $V_u$  = the signal strength vector from the user terminal;  
 $M_d$  is the mean distance between the vector obtained by the user terminal and the vector at the  $d$ th position in the database;  
 $d_{max}$  is the number of measurement positions;  
In this paper, this value is equal to 35;  
 $f_{max}$  is the amounts of data at the same location;  
In this paper, this value is equal to 7;  
 $|X|$  = the norm of the vector  $X$ ;  
 $d = 1, 2, \dots, d_{max}$ .

### 3.5 Mapping

The purpose of the mapping step is to convert the vector difference 3.4 to the actual spatial position coordinates. Based on the vector differences  $M_1, M_2, \dots, M_{d_{max}}$ , the two smallest values  $M_{mina}, M_{minb}$  were calculated. The corresponding two-dimensional spatial coordinates  $(x_{mina}, y_{mina})$  and  $(x_{minb}, y_{minb})$  were used for the following calculations. The location of the user terminal is calculated with the following formula:

$$\begin{aligned} x_u &= \frac{B}{A+B} \cdot x_{mina} + \frac{A}{A+B} \cdot x_{minb}; \\ y_u &= \frac{B}{A+B} \cdot y_{mina} + \frac{A}{A+B} \cdot y_{minb}. \end{aligned} \quad (8)$$

where  $V_u$  is the signal strength vector from the user terminal  
 $M_d$  is the mean distance between the vector obtained by the user terminal and the vector at the  $d$ th position in the library  
 $|X|$  = the norm of the vector  $X$   
 $d = 1, 2, \dots, d_{max}$   
 $A = 10^{M_{mina}}$   
 $B = 10^{M_{minb}}$

## 4. INDOOR FIELD TESTS

### 4.1 Indoor Environment

The location for indoor field testing in this paper was a lounge. As shown in Figure 7, the test area was a rectangle 6.4 m long and 4.8 m wide. The audio signal base station was in the middle of the rectangle and was 2.3 m high. The user terminal was placed at a height of 1.2 m and evaluated. The different launch directions of the base stations were also indicated in Figure 7.

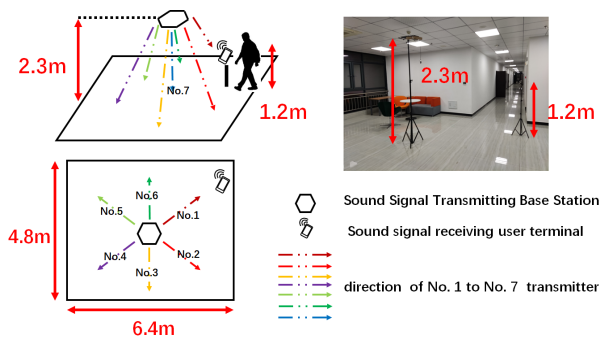


Figure 7. Indoor environment and base station deployment

According to Section 3.4, it is necessary to collect data from multiple sampling points in the test area and build a library database. Figure 8 depicts the location of the sampling point and the test area.

Since the audio signal strengths from different audio transmitters are the same but the transmission directions are different, the audio signal strengths from the same audio transmitter will vary in diverse locations. The distributions of 19Khz audio signal strength from the transmitter and background noise at distinct locations in the test area are shown in Figure 9.

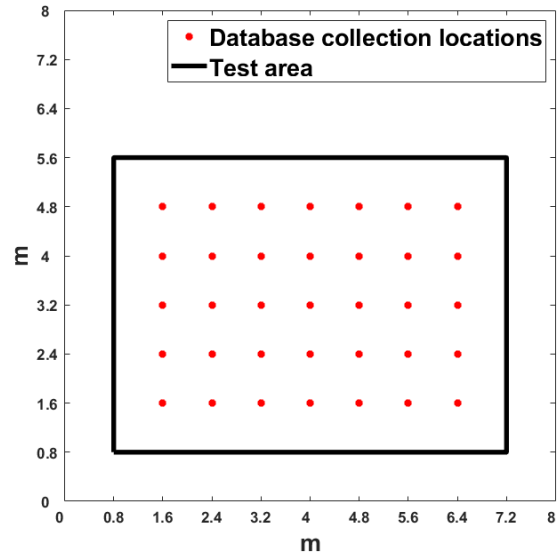


Figure 8. The location of the sampling point and the test area.

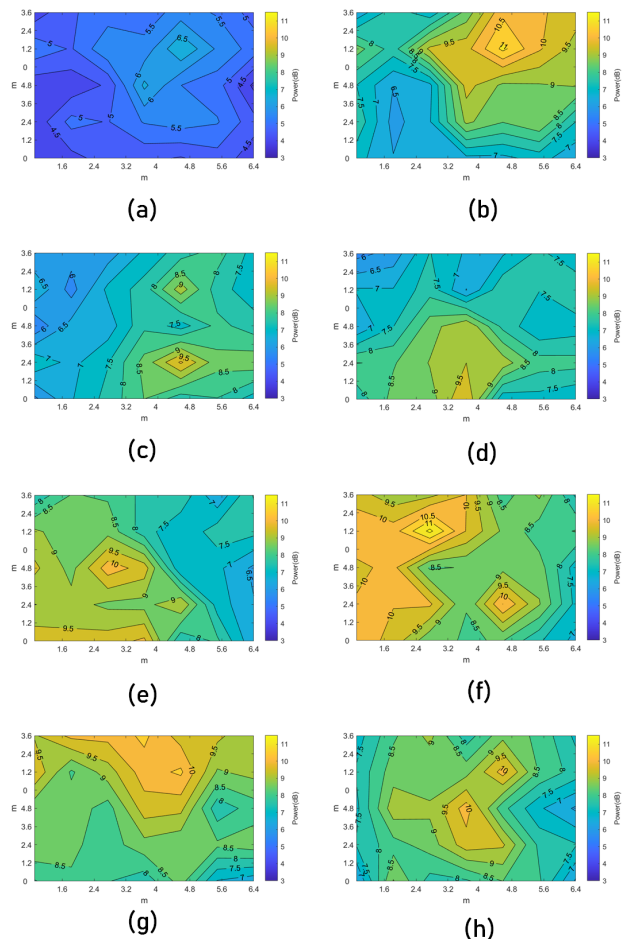


Figure 9. The distribution of 19Khz signal strength in the test area (a) The background noises (b) - (h) The signal from the No.1- No.7 transmitters.

## 4.2 Static Tests

In the static tests, twenty-five points in the area were evaluated. Parts of real point and measured point and the CDF of error are shown in Figure 10. In the static test, RMSE is 0.82m and MAE is 0.51m.

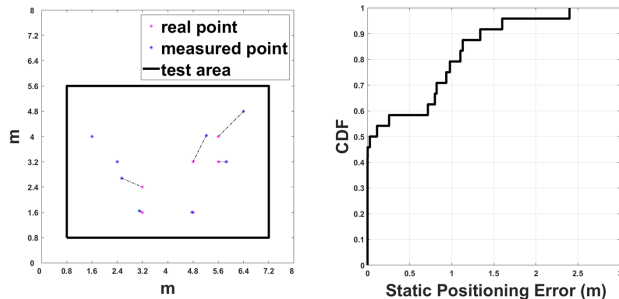


Figure 10. Static positioning and the CDF of error.

## 4.3 Dynamic Tests

The data processing flow of dynamic testing is the same as that of static processing. The first step is to divide a piece of data collected during continuous dynamic motion into multiple frames. The second step is to process and position the data of different frames. The last step is to acquire the path between multiple locations as the measurement path. In the dynamic test, RMSE is 0.86m and MAE is 0.70m. The dynamic test path in this article is a “L”-shaped path. Figure 11 shows the real path and the measured path of the dynamic test and the CDF of positioning error.

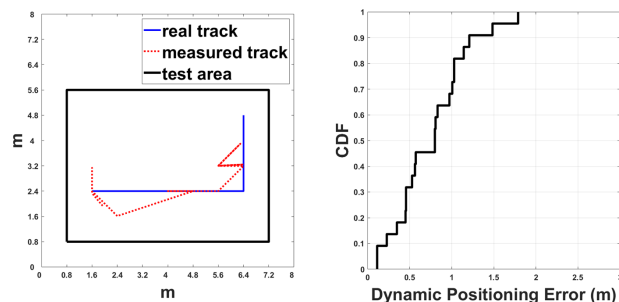


Figure 11. Dynamic positioning and the CDF of error.

## 5. CONCLUSION

The purpose of this paper is to propose an audio positioning method based on a single base station audio signal for solving the indoor positioning problem in current technology. The signal receiver analyzes the strength of the audio signal emanating from the base station’s various directions. For difference calculations, the audio signal strengths are viewed as a vector and compared to the database vector. Finally, the receiver’s spatial position information is determined using the spatial position mapping relationship. In the future, we will investigate the relationship between the number of signal transmitters on the base station and the positioning accuracy, as well as the large area positioning scheme, using the findings from this paper.

## ACKNOWLEDGEMENTS

This research is supported by Special Fund of Hubei LuoJia Laboratory under grant to no. 220100008, the National Natural Science Foundation of China under Grant 42171417, the Key Research and Development Program of Hubei Province under grant number 2021BAA166, and the Special Research Fund of LIESMARS.

## REFERENCES

- Al-homayani, F., Mahoor, M., 2018. Improved indoor geomagnetic field fingerprinting for smartwatch localization using deep learning. *2018 International Conference on Indoor Positioning and Indoor Navigation (IPIN)*, 1–8.
- Chen, L., Lu, X., Shen, N., Wang, L., Zhuang, Y., Su, Y., Li, D., Chen, R., 2021a. Signal Acquisition of LuoJia-1A Low Earth Orbit Navigation Augmentation System with Software Defined Receiver. *Geospatial Information Science*, 1 - 16.
- Chen, L., Thombre, S., Jarvinen, K., Lohan, E. S., Alen-Savikko, A. K., Leppakoski, H., Bhuiyan, M., Bu-Pasha, S., Ferrara, G. N., Honkala, S., 2017. Robustness, Security and Privacy in Location-Based Services for Future IoT: A Survey. *IEEE Access*, 1-1.
- Chen, L., Zhou, X., Chen, F., Yang, L.-L., Chen, R., 2021b. Carrier Phase Ranging for Indoor Positioning with 5G NR Signals. *IEEE Internet of Things Journal*, 1 - 1.
- Chen, R., Chen, L., 2021. Smartphone-Based Indoor Positioning Technologies. *Springer Singapore*, 467-490.
- Farahsari, P. S., Farahzadi, A., Rezazadeh, J., Bagheri, A., 2022. A Survey on Indoor Positioning Systems for IoT-based Applications. *IEEE Internet of Things Journal*, 1-1.
- Ji, T., Li, W., Zhu, X., Liu, M., 2022. Survey on indoor fingerprint localization for ble. *2022 IEEE 6th Information Technology and Mechatronics Engineering Conference (ITOEC)*, 6, 129–134.
- Li, Z., Su, Z., Yang, T., 2019. Design of intelligent mobile robot positioning algorithm based on imu/odometer/lidar. *2019 International Conference on Sensing, Diagnostics, Prognostics, and Control (SDPC)*, 627–631.
- Liang, C., Lie-Liang, Y., Jun, Y., Ruizhi, C., 2017. Joint Wireless Positioning and Emitter Identification in DVB-T Single Frequency Networks. *IEEE Transactions on Broadcasting*, 63(3), 577 - 582.
- Pakanon, N., Chamchoy, M., Supanakoon, P., 2020. Study on accuracy of trilateration method for indoor positioning with ble beacons. *2020 6th International Conference on Engineering, Applied Sciences and Technology (ICEAST)*, 1–4.
- Shen, N., Chen, L., Lu, X., Ruan, Y., Hu, H., Zhang, Z., Wang, L., Chen, R., 2022. Interactive multiple-model vertical vibration detection of structures based on high-frequency GNSS observations. *GPS Solutions*, 26(2), 1 - 19.
- Shen, N., Chen, L., Wang, L., Hu, H., Lu, X., Qian, C., Liu, J., Jin, S., Chen, R., 2021. Short-Term Landslide Displacement Detection Based on GNSS Real-Time Kinematic Positioning. *IEEE Transactions on Instrumentation and Measurement*, 70, 1-14.

Shilo, G., Romaniuk, D., Pysarskyi, A., Lebedieva-Dychko, A., 2020. Cost-effective indoor positioning using iot solutions. *2020 IEEE 5th International Symposium on Smart and Wireless Systems within the Conferences on Intelligent Data Acquisition and Advanced Computing Systems (IDAACS-SWS)*, 1–5.

Soda, S., Kugata, K., Takagi, T., Noguchi, H., Izumi, S., Yoshimoto, M., Kawaguchi, H., 2011. Positioning system for mobile terminals using a microphone array network as an intuitive interface. *2011 Joint Workshop on Hands-free Speech Communication and Microphone Arrays*, 155–156.

Song, S., Feng, F., Xu, J., 2020. Review of geomagnetic indoor positioning. *2020 IEEE 4th International Conference on Frontiers of Sensors Technologies (ICFST)*, 30–33.

Wang, Z., Chen, R., Xu, S., Liu, Z., Guo, G., Chen, L., 2015. A Novel Method Locating Pedestrian With Smartphone Indoors Using Acoustic Fingerprints. *IEEE Sensors Journal*, 21(24), 27887 - 27896.

Yao, L., Wu, Y., Yao, L., Liao, Z. Z., 2017. An integrated imu and uwb sensor based indoor positioning system. *2017 International Conference on Indoor Positioning and Indoor Navigation (IPIN)*.

Yu, Y., Chen, R., Shi, W., Chen, L., 2022. Precise 3D Indoor Localization and Trajectory Optimization Based on Sparse Wi-Fi FTM Anchors and Built-in Sensors. *IEEE Transactions on Vehicular Technology*, 1-1.